MATERIALS AND INTERFACES

Effect of Polymer Granules on the Electrostatic Behavior in Gas−Solid Fluidized Beds

Xianbo Yu, Wei Li, Yi Xu, Jingdai Wang,* Yongrong Yang, Nan Xu, and Haoqi Wang

State Key Laboratory of Chemical Engineering, Department of Chemical and Biochemical Engineering, Zhejiang University, Hangzhou 310027, People's Republic of China

Granules polymers electrostatic behavior in a fluidized bed can be complicated by the differences in catalyst residue and surface properties among them. Electrically charged particles cling together in large aggregates and adhere to the wall of the apparatus. Polymer particles with the same chemical composition but different sizes would have their own special contributions to the generation of static charges. It is improtant to understand polymer particles role on electrostatic charge generation and dissipation. Experiments are carried out in a gas−solid fluidized bed with nitrogen as the fluidization gas to determine the relationship between the electrostatic charge level and the size of the polyethylene granule. By measuring the electrostatic potentials at different bed axial heights, it is found that the electric field inside the bed is significantly influenced by the size, weight fractions, and catalyst residue of added granular polyethylene. Consequently, an impact factor of granules (F_b) is proposed to study the influence of particle size and the weight percent of the residual catalyst to the electrostatic potentials. And it is found that the greater the degree of fineness of the granules, the more percentage of the residual catalyst in the particles, which results in the stronger affect on the electrostatic behavior in the fluidized bed.

1. Introduction

The most widely established industrial gas-phase technology for polyolefin production is the fluidized bed.[1,2] Fluidization of polymer powders is an initial stage in most powder-related processes, and electrostatics plays a role in this fluidization. The first references on the presence of triboelectrification of particles in a fluidized bed appeared in the late 1940s and early 1950s.[3−6] Several researchers began to notice anomalous electric behavior in different studies using fluidized bed.[3−6] The electrostatic charging of powders can occur naturally or artificially. The accumulation of resultant charges on system components may cause electrostatic hazards which hamper the desired pneumatic conveying process.[7,8] Electrostatics can represent a serious problem for fluidized beds, causing agglomeration, nuisance discharge, and even the danger of explosions.[9−14] Charging in a fluidized bed was considered to be more of a nuisance rather than useful.[3−6]

Solid particles in a pneumatic transport system are naturally charged because of collision with surfaces of different materials. The mechanism is quite complex.[15] Electrostatic effects inside a fluidized bed are due to continual particle−particle and particle−wall collisions that result in the tribocharging or friction charging of the powder particles.[16] It has been observed that not only tribocharging occurs in the fluidization of insulating particles but induction charging also occurs in the present study. Contact charging between particles with different sizes results in larger particles gaining an opposite polarity of charge compared to smaller particles,[17,18] resulting in bipolar charging.[17−24] Thus, the size of the particles in the fluidized bed played an important role during the charging.

Gardiola investigated the relationship between the degree of electrification and the variable of particle diameter.[15,25] It was found that the degree of electrification increased with the particle size. Moreover, it was found that the addition of granular particles could reduce the accumulation of the electrostatic charges in fluidized beds according to the literature.[26−30] Mehrani et al.[31] added various fine particles to a gas−solid fluidized bed and found that the entrained fines carried significant amounts of charge out of the fluidization column, which disturbed the equilibrium of charge in the fluidized bed. In addition, they conducted a preliminary study on the electrostatic characteristic of particles of the same material but different sizes.

Particle size plays an important role in the process of the electrostatic charging in gas−solid fluidized beds. Nevertheless, there have been few systematic studies on the electrostatic characteristic of the system for particles of the same material but of different sizes, especially on the electrostatic effect of granular particles on fluidization. Besides, the variable of particle size should not be left to itself, and it has relation to some other variables. The catalyst particles break into fragments during polymerization.[32] Furthermore, it has been reported that polymer particles of different sizes will vary in properties, including different molecular weight, copolymer content, surface roughness, and the amount of residual catalyst. And these can alter the work function and the charging characteristics of particles.

In this study, experiments are carried out in a three-dimensional column gas−solid fluidized bed by adding material identical to the bed material but in different amounts and particle sizes in order to simplify the understanding of electrostatic charge generation and dissipation. In particular, the effects of particle size and the residual catalyst in the polyethylene powder are investigated simultaneously.

* To whom correspondence should be addressed. E-mail: wangjd@zju.edu.cn.

10.1021/ie8017077
Published on Web 12/01/2009

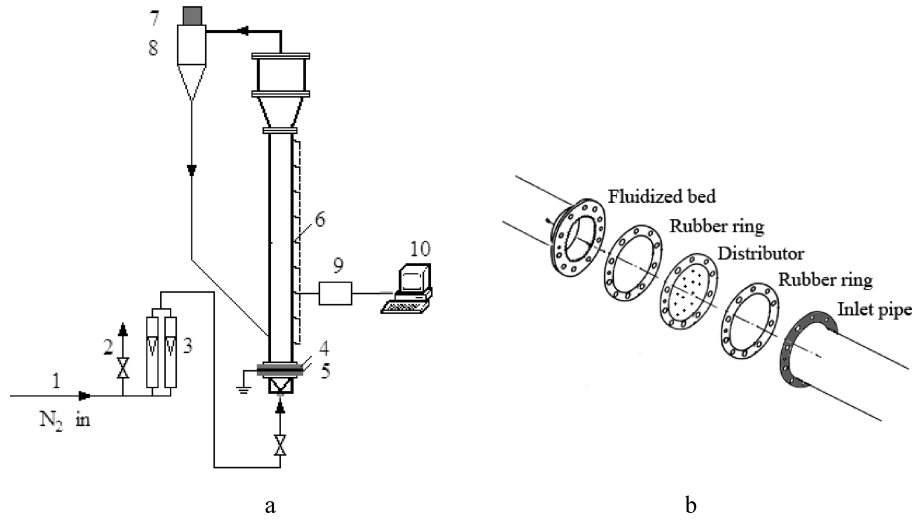

Figure 1. Diagram of fluidized bed experimental apparatus ((a) apparatus; (b) details in the insulation): (1) N_2-in pipeline; (2) vent valve; (3) flow meter; (4) rubber ring (leakage proof seal); (5) distributor; (6) measuring points; (7) filter bag; (8) cyclone; (9) signal transmitter; (10) computer and data acquisition system.

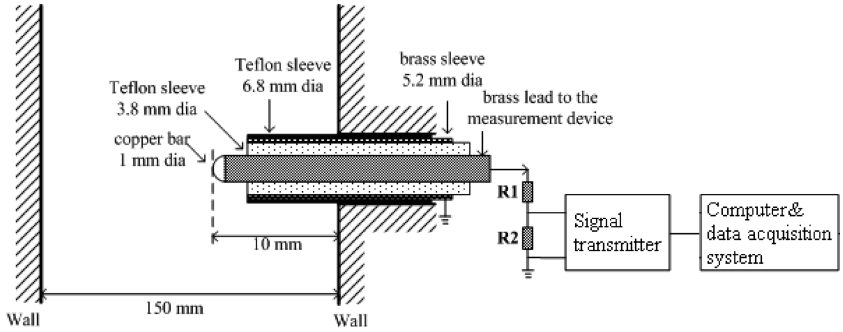

Figure 2. Schematic of electrostatic ball probe and electric circuit.

2. Apparatus and Fluidization Experiments

2.1. Experimental Apparatus. Fluidized Bed. The experiments are carried out in a three-dimensional Plexiglas fluidized bed, as shown in Figure 1a (0.15 m in inner diameter and 1.0 m in height). A rubber is used at the bottom to keep a good seal and prevent leakage, shown in Figure 1b. The gas distributor is a stainless steel perforated plate with a pore diameter of 2.0 mm and an open area ratio of 2.6%. The distributor is grounded during fluidization experiments to eliminate external electric interference. The expansion section is connected to a cyclone at the top of the bed. A filter bag is used to collect the fine. The heavier particles are returned to the bed from the bottom of the cyclone.

The relative humidity of the fluidizing gas strongly affects the dissipation of electrostatic charges in the fluidized bed.[9,15] Any change in temperature results in a change in humidity. Therefore, both the relative humidity and the temperature of fluidizing gas are under control during the experiments. Dry nitrogen (purity, 99.99%) serves as the fluidizing gas to eliminate humidity and contamination effects that might affect the generation of charge inside the fluidized bed. All experiments are performed at 25 °C.

Potential Online Detection and Details. An electrostatic potential online detection (EPOD) system consistes of three parts: a single movable electrostatic potential sensor, data collection system, and data output system. Several measuring points at various heights along the column are connected to a static probe (shown in Figure 2). The probe is comprised of a copper bar and hemisphere sensing surface (1 mm in diameter). The probe is with a Teflon and brass sleeve immersed in the fluidized bed (from the wall). Compared to the bed diameter (150 mm), the probe is regarded as a point sensor since the static probe has a small (1 mm) diameter and most of the probe is covered with a small area exposed in the bed. The Teflon sleeve is used to insulated to the ground, and this Teflon tube is enclosed by a brass sleeve to reduce the background current due to buildup of charge on the walls of the column. The outer diameter of the Teflon sleeve is 6.8 mm in order to fit into the ports on the column, and this insulating material prevents charge leakage

The voltage measuring system includes the following: a static probe, a 4×10^{11} Ω resistor (Ohmite, USA/MOX 1125-23JE), a variable-resistance and a voltage to current transducer (ADTECH, USA/MVX-106) with direct current (DC) power supply. The data collection system consists of a data acquisition card (NI, USA/PCI-6071E). A computer installed with the program Labview comprises the data output system.

Fines Injection System. The fines injection system is shown in Figure 3. The fines are injected though a tube near the distributor using flowing nitrogen gas. Friction between the fines and the tube charge the particles into the bed. As a limitation, the accumulation of total charge in the bed at a given time could not be measured. We put the electrostatic probe near the injection port and find that the potential drops to zero over time gradually. Likewise charge is consumed gradually within several minutes when injected through the tube into a small Faraday

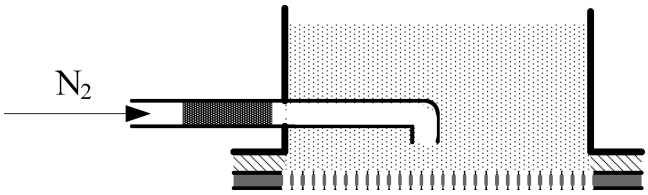

Figure 3. Diagram of fines injection system.

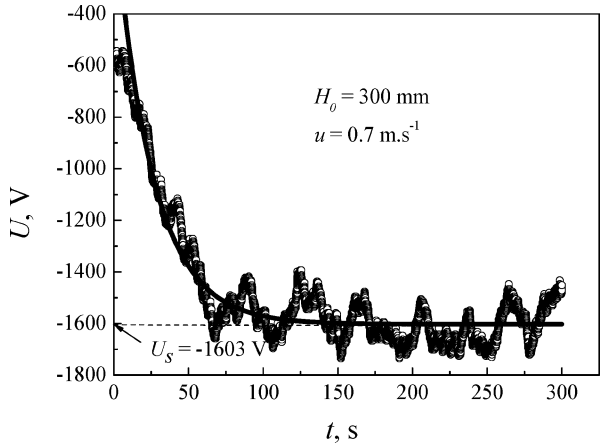

Figure 4. Raw signals of electrostatic potentials (H_e=160 mm).

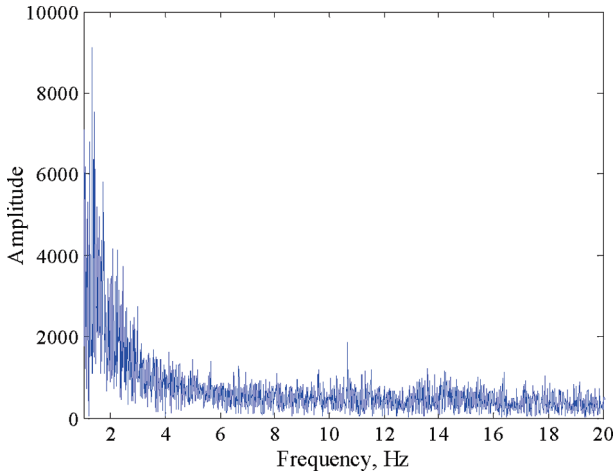

Figure 5. FFT (fast Fourier transformation) of the electrostatic potential signal (H_0 = 300 mm, u = 0.7 m·s^{-1}, and H_e = 160 mm).

cup. Consequently, after the injection of fines, 10 min is needed to consume the charges carried into the bed so as not to affect the results.

Implementation Details. The basic principle of choosing sample frequency for a detection technique is that a relatively low sample frequency is preferred on the condition that no information of the signals is left.

The sampling rate should be fast enough (more than two times) to record all frequencies according to the Nyquist−Shannon sampling theorem. On the other hand, working at lower sample frequency avoids digital processing of a large-scale time series and spans the number of data processing techniques that can be applied over digital. A raw data of electrostatic potentials is shown in Figure 4. Figure 5 shows the fast Fourier transformation (FFT) of the raw electrostatic potential signal of linear low-density polyethylene (LLDPE). It shows prominent frequencies at approximately 0−16 Hz. All of the signal energy is concentrated below 20 Hz, meaning that the sample frequency of 100 Hz is high enough to record all information from the signals.

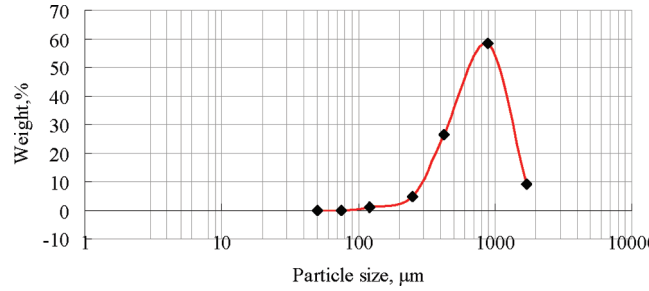

Figure 6. Particle size distribution of LLDPE.

Table 1. Properties of LLDPE Particles

particle type	MI,[a] g·(10 min^{-1})	P, g·cm^{-3}	$\bar{d}_p$, μm	residual catalyst,[b] wt %
CP	2.0	0.92	1275	0.026
GP1	2.0	0.92	855	0.028
GP2	2.0	0.92	620	0.032
GP3	2.0	0.92	402	0.034
GP4	2.0	0.92	185	0.050

[a] Melting index of LLDPE particles, g·(10 min^{-1}). The value of the melting index is measured by the supplier (Sinopec, China Petroleum & Chemical Corp.). [b] In the process of polymerization, the polymer grows around the catalyst particles with catalyst particles left in the polyethylene particles, which are called residual catalyst. The weight percent of the residual catalyst refers to the mass fraction of the residual catalyst in the polyethylene particles. The value of residual catalyst is measured by the supplier (Sinopec). The measurement is based on the National Standard Inspection—determination of the ash content is by incineration.

The sampling time should be long enough to reach the steady-state potential, so 300 s is adopted as the sampling time.

2.2. Experimental Method. The diameter range of particles used in the experiments is determined by sieving received LLDPE from the supplier (Sinopec, China Petroleum & Chemical Corp.). A typical particle size distribution is given in Figure 6. The coarse particles (CP) are used as the main fluidized particles, while the granular polyethylene GP1, GP2, GP3, and GP4[34] are the particles added in different weight percents shown in Table 1. All polyethylene particles tested have the same MI (melting index) and density. LLDPE powder samples are dried before each run to eliminate humidity and contamination effects.

The measuring points in Figure 1, H_e, are as follows: 80, 160, 245, 380, 515, and 650 mm as measured from the distributor for a static bed level (H_0 = 200 mm) at the superficial velocity (u = 0.7 m·s^{-1}, bubbling fluidization). At first, electrostatic potentials using only fluidized CP are measured. Granular polyethylene is added in different weight percents at the same total bed mass, and the corresponding electrostatic potentials are detected when a steady state is reached.

3. Results and Discussion

3.1. Electrostatic Potentials after Injection. Electrostatic Potentials at Different Injection Amounts. The weight percent of the granules in the bed is increased from 1% to 23%. The electrostatic potentials outputs for different particles are different.

Figure 7 shows the experimental results for the change in electrostatic potentials after the injection of granular polyethylene with different weight percents.

For GP4 (185 μm, $\bar{d}_p$), it is quite different and significant. When $\omega_{GP4} < 3\%$, the static potentials almost stay the same as the addition of the granules increases. In the range $3\% < \omega_{GP4}$

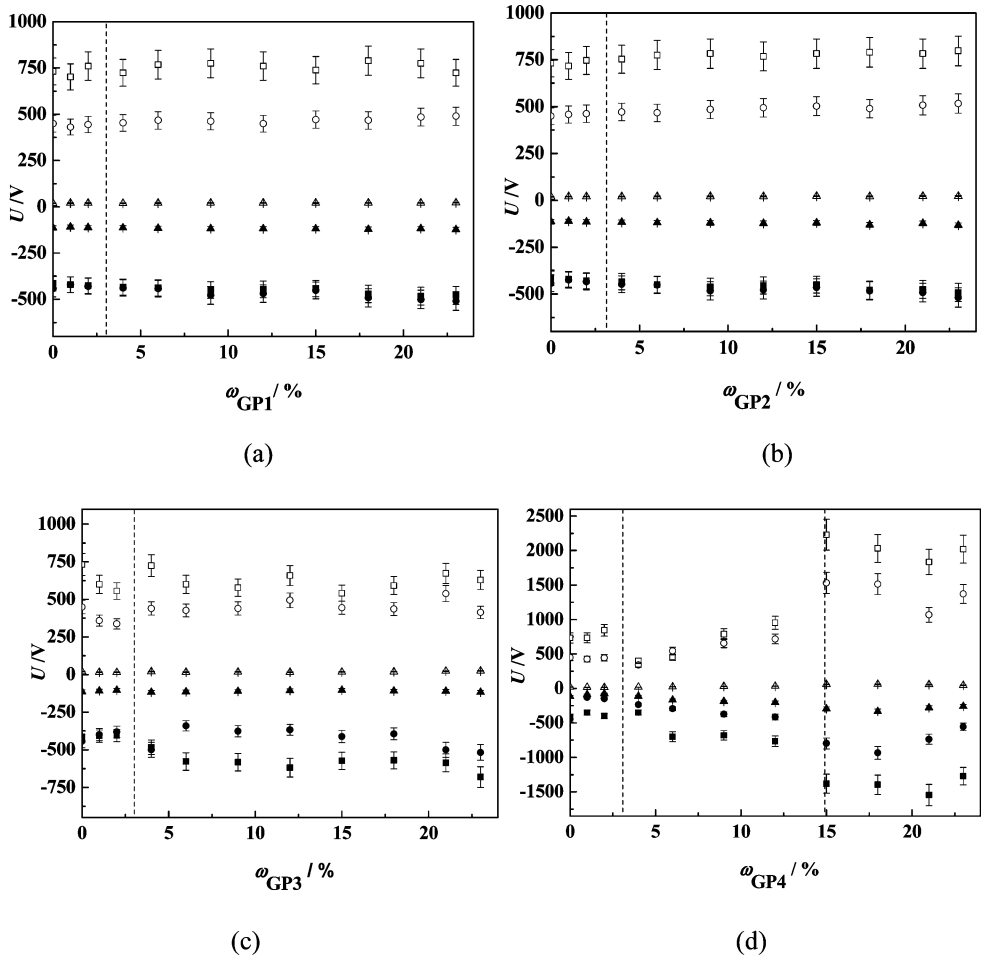

Figure 7. Changes of electrostatic potentials in the fluidized bed with different weight percent particles added: H_e = (■) 80, (●) 160, (▲) 245, (□) 380, (○) 515, and (Δ) 650 mm. The electrostatic potentials were measure in the gas−solid fluidized bed at the heights of 80, 160, 245, 380, 515, and 650 mm with different sizes and weight percents of granular polyethylene added: (a) GP1 particles, (b) GP2 particles, (c) GP3 particles, (d) GP4 particles, from 1% to 23%. The static bed level H_0 = 200 mm, and the superficial velocity u = 0.7 m·s^{-1}. The error bar in a−d indicate the deviation for five experiments.

< 15%, rapid increase of the electrical potentials appears and then it shows a downward trend. The adding of GP4 particles resultes in the electrostatic potentials shifting from hundreds to thousands. The large error bars indicate that the charge dissipation is highly unstable when the injection amount exceeds 15%.

For GP3 (402 μm, $\bar{d}_p$), it is a little different. The potentials show the same when the weight percent of GP3 particles is less than 5%. An increasing trend and then fluctuation in the electrostatic potentials is observed with further injection, indicating more charge accumulation and dissipation in the fluidized bed.

For GP1 (855 μm, $\bar{d}_p$), the potentials remain the same at hundreds of volts with the injection increases. For GP2 (620 μm, $\bar{d}_p$), the potential signals are steady, which is similar to those of GP1. The electrostatic potentials with hundreds of volts remain quite constant as the injection amount of GP2 is increased from 1% to 23%. The further addition of GP1 or GP2 particles does not affect the electrostatic potential in the bed.

The experiment represents some different results from the previous research.[9−11] The electrostatic potentials decrease at low addition amount. However, a rapid increase of the electrostatic level in the bed is observed at further injection. It is found that the electrostatic potentials remain at low level when the amount of granules added is small, but it leads to a high potential at thousands of volts if the granules in the bed are increased.

Electrostatic Potentials at Different Locations. The result of electrostatic potentials versus height is shown in Figure 8. The addition of GP4 resultes in obvious changes in the electrostatic potentials. The shape of the electrostatic potential versus height remains the same and becomes wider. The absolute values of electrostatic potentials at the bottom and top of the bed both increase, indicating that the electrostatic charges are accumulated in the whole bed. The injection of GP1 or GP2 causes fluctuation within the small range of the electrostatic potentials, and the Z-shaped potential distribution gradually grows wider as the amount of GP3 is added in.

Conservation of Electric Charge. The electrification charges including the positive charges and negative charges are separated due to the particle contact and separation. Some of the particles possess more positive charges than before and some possess more negatives charges, and the net charge is almost zero. The net charges do not almost change although both the absolute values of the negative charges and positive charges increase. However, particles with the different sizes have different resident time in the fluidized bed, especially for a small quantity of the small size particle for elutriation and circulation. And the particle size distribution changes with the location of the fluidized bed. Besides, the extent and rate of charge generation and dissipation change in different locations of the fluidized bed. All of these factors result in the nonconservation of electric charge in certain local areas of the fluidized bed, but the electric charge is conserved for the whole fluidized bed, and the net charge is

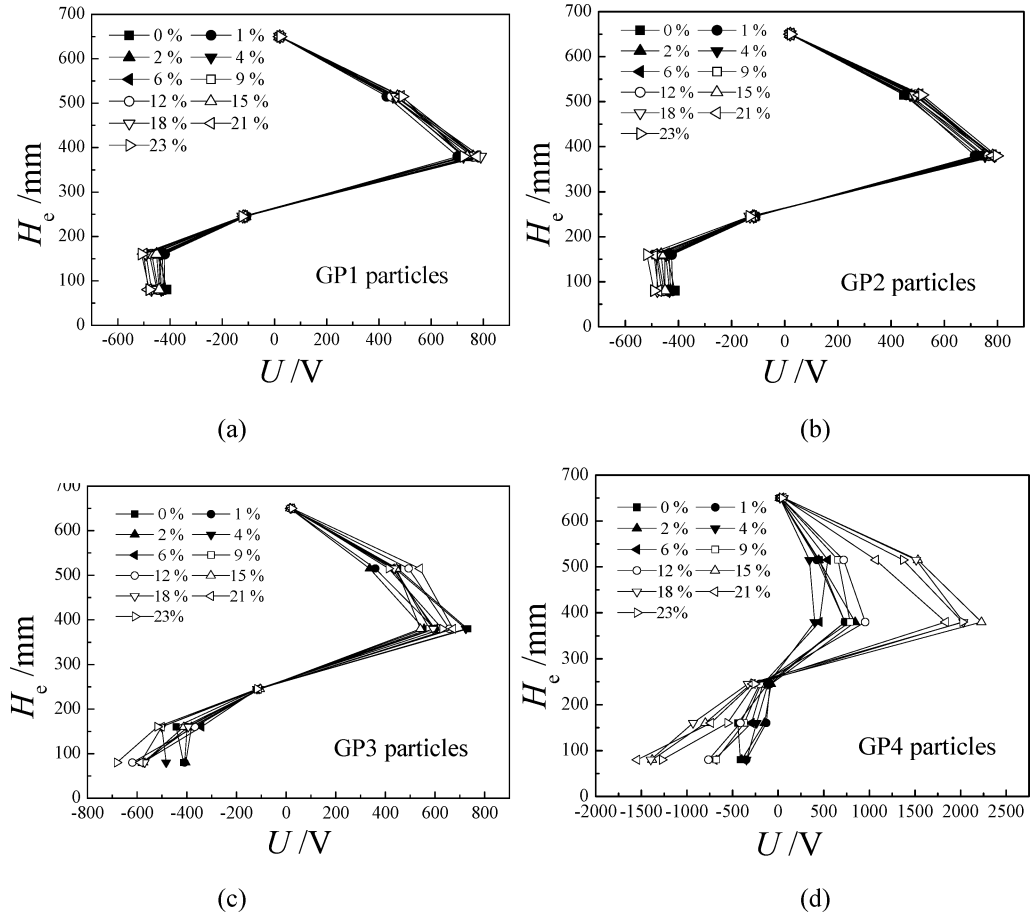

Figure 8. Electrostatic potential versus height as the granular injection increased: (a) GP1 particles, (b) GP2 particles, (c) GP3 particles, and (d) GP4 particles. Error bars in a−d have been omitted for readability.

almost zero. In addition, the measurement errors occurr randomly due to the instruments and sensors and the net charge is not equal to zero.

3.2. Impact Factor of Granular Particles (F_b). The polymer grows around the catalyst active sites during the polymerization. Some of the catalyst sites are left in the polyethylene particles when the polymerization is terminated. The more fully the LLDPE chains grew, the less residual catalyst there would be. However, these residual catalysts provided steps for the electrons transition. Different sizes of LLDPE particles have the different weight percents of the residual catalyst and different numbers of local energy level, which results in the diverse work function, transition capability, and numbers of the transit electrons. Besides, the differences of particle sizes influence the hydrodynamic behaviors, contact mode, and area between the particles. Thus, the different sizes of particles have different effects on the electrostatic potentials in the fluidized bed. The LLDPE particles used in the experiment have no difference among each other except the particle size and the weight percent of residual catalyst. The granules influence factor F_b is proposed according to the above results. F_b is composed of the particle size influence factor F_b' and the residual catalyst influence factor F_b''.

$$F_b = F_b' \times F_b'' = \left(\sum_i \frac{\overline{d_P}\omega_{GPi}}{d_{GPi}} \right)^2 \left(\sum_i \frac{c_{GPi}\omega_{GPi}}{c_{CP}\omega_{CP} + c_{GPi}\omega_{GPi}} \right) \quad (1)$$

Figure 9 is the granules influence factors for each particle in a limited range we investigate. F_b decreases as the particle size increases, and F_b increases as the weight percent of residual catalyst increases. All the factors F_b are less than 0.1 in GP1, GP2, and GP3. The F_b of GP4 is much more sensitive to the weight percent of the residual catalyst and is much more than that of GP1, GP2, or GP3 as the injection increases.

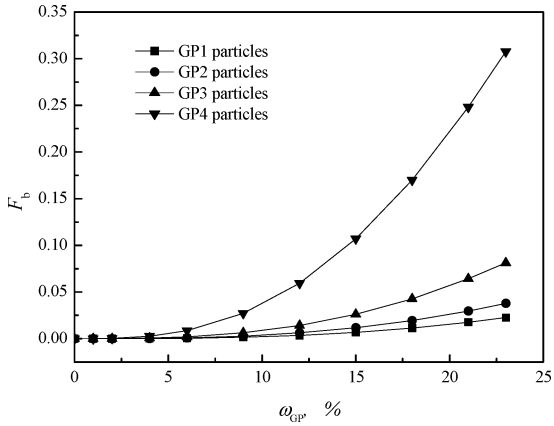

Figure 9. Relationship between F_b and weight percent of granular particles with different sizes: (■) GP1 particles, (●) GP2 particles, (▲) GP3 particles, and (▼) GP4 particles. Granules influence factor F_b was proposed, composed of particle size influence factor F_b' and residual catalyst influence factor F_b'' to explain the weight percent of residual catalyst and the size effect of the granules.

The electrostatic potential versus granular influence factor is shown in Figure 10. The electrostatic potentials remain the same when $F_b < 0.025$. And the electrostatic potentials increase with the injection amount when $0.025 < F_b < 0.05$. A rapid increase

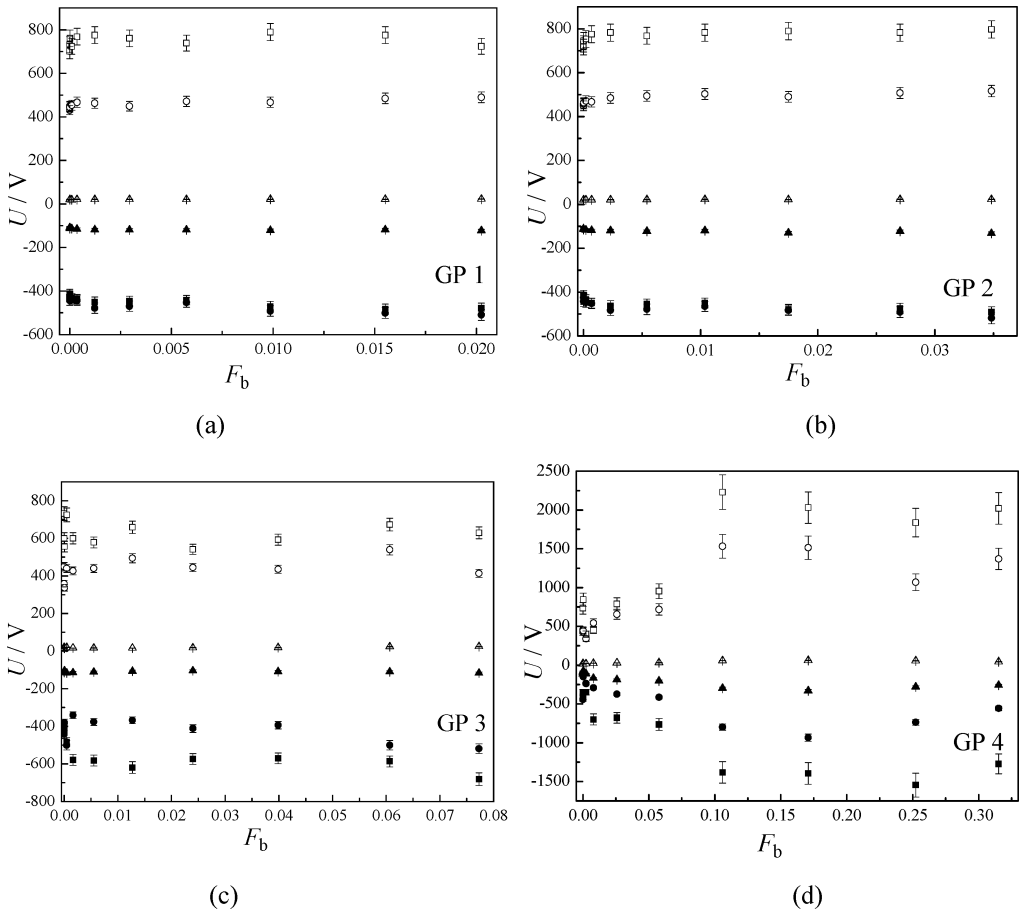

Figure 10. Electrostatic potential versus granular influence factor as the granular injection increased: H_e = (■) 80, (●) 160, (▲) 245, (□) 380, (○) 515, and (Δ) 650 mm; (a) GP1 particles, (b) GP2 particles, (c) GP3 particles, and (d) GP4 particles.

of electrical potential appears and then shows a fluctuation trend since F_b exceeds 0.05.

3.3. Effect of Electrostatic Charge Transfer and Accumulation of Granular Particles. Model of Granules Effect in the Fluidized Bed. The granules effects on the changes of electrostatic charges were explained by two main aspects. On one hand, the difference of particle size and surface meant the dissimilar contact surface and contact mode among particles. On the other hand, different weight percents of residual catalyst provided diverse local energy levels for the electrons transition.

The contact charges are proportional to contact surface.[28,35−37] The larger difference between the size of the coarse particles and granules results in the greater influence on the contact area. The contact area has more effect on the charge generation, transfer, and accumulation because the quantity of the transferred charges is proportional to the contact area between particles. The electric forces in the bed with an admixture of granules are different from those in the bed of pure polyethylene.

The effect of the granules on the contact mode was illustrated in Figure 11. Two types of possible contacts can be expected: the contact between the coarse particles themselves (C−C) and between coarse particles and the wall surface (C−W). Then, the contact between the coarse particles and granular polyethylene-(C−G) and between granular polyethylene and the wall surface (G−W) increases by the presence of some granular particles into the bed. The granular particles are attracted on the surface of the coarse particles, which limits the contacts of C−C and C−W. The contacts of G−G and G−W become the leading contact mode as the injected granule amount increases, and the contact types C−C and C−W are hindered. As a result, the contact surfaces between particles which generated charges are

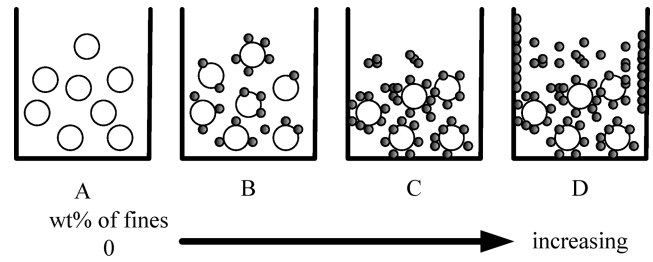

Figure 11. Transition of the bed structure with the increase of granular polyethylene added in the fluidized bed (only coarse particles included).

reduced. As the amount of granules increases the contact between G−G and G−W increases; then it goes out of a certain range.

Charge Transfer and Accumulation by Granules in the Fluidized Bed. For GP4 (185 μm, $\bar{d}_p$), it is quite different. First the contacts of C−C and C−W are decreased, while C−G and G−W are increased due to the presence of some granular particles into the bed. The contact types C−C and C−W are hindered as the amount of granules increases. However, the contact of G−G and G−W become the leading contact mode. Therefore, charges generated from the contact surfaces between particles C−C are reduced. Charge transfer and accumulation are mainly from G−G and G−W. The electrostatic potentials continued to increase until the inside surface of the wall is covered with granular particles and the majority of coarse ones attract a lot of granules. Since then the dominant contact mode is the G−G contact, and the electrostatic potentials begin to drop. However, this situation should be avoided, because the

severe status of particle adhesion to the wall would cause sheeting on the wall easily in the industrial polymerization reactor.

For GP3 (402 μm, $\bar{d}_p$), it is a little different. Residual catalyst and particle size simultaneously influence the electrostatic potentials in the fluidized bed when GP3 particles are added. some are attracted on the surface of the coarse particles when a small amount of granular polyethylene is added. On one hand the C−C and C−W contacts are partially blocked and reduced; on the other hand coarse particles and granules charge oppositely due to different work function.[38] Thus, the charges on the particles are neutralized when the granular polyethylene is attracted on the coarse particles. Accordingly, the charge accumulation in the bed reduces at low feed of granular polyethylene. The electrostatic potentials increase gradually as the feed amount increases, because the increase rate of charge by contact areas exceeds the rate of charge by neutralization.

For GP1 (855 μm, $\bar{d}_p$) and GP2 (620 μm, $\bar{d}_p$), the changes in contact area and charge transferred are not obvious. Consequently, these two kinds of particles have an unapparent effect on the charge accumulation and electrostatic potentials in the fluidized bed.

The experimental results also shows that electrostatic potentials are different at different measurement heights. The value of the electrostatic potential at $H_e = 80$ mm represents the biggest of the three measurement points. This is mainly due to the different character of charge generation and accumulation in different heights of the bed, including the bipolar charging, the bed particle size segregation, and the hydrodynamics behavior. After contact and friction, some of the granular polyethylene is carried to the upside of the bed and leaves the coarse ones charged oppositely. And the rapid change of concentration of coarse particles, particles, and bubble movement at the measurement position on the condition of bubbling fluidization lead to the variety of the electrostatic potentials.

4. Conclusions

Experiments are carried out in a cold-model three-dimensional fluidized bed with nitrogen as the fluidization gas. The effect of the granules on the electrostatic potential is studied via adding different sizes of granular LLDPE particles to the same coarse ones.

(i) Addition of big size granules in a fluidized bed results in no apparent effect on the electrostatic level other than a little fluctuation of the electrostatic potentials. Injection of small size granules to the fluidized bed would be complicated. The electrostatic potentials stay the same and then increase rapidly when the amount of fines is small. The electrostatic potentials fluctuate and then drop slightly as the amount of fines increases. Moreover, the greater degree of fineness of the granules, the stronger influence of it on fluidized bed behavior.

(ii) A greater percentage of the residual catalyst in the particles results in a stronger affect on the electrostatic behavior in the fluidized bed.

(iii) The mechanism of the process consists of a change of contact mode between particles (C−C, C−W, G−G, G−W, and C−G) in the bed and in the generation, transfer, and neutralization of electrostatic charge by granules.

Acknowledgment

The authors acknowledge the support and encouragement of the National Natural Science Foundation of China (Grant Nos. 20490205, 20676114, and 20736011) and the National High Technology Research and Development Program of China (Grant No. 2007AA030208).

Nomenclature

c_{GPi} = weight percent of residual catalyst in GP*i* polyethylene, %
c_{CP} = weight percent of residual catalyst in CP polyethylene, %
$\bar{d}_p$ = average size of mix particles, μm
d_{GP} = average size of GP*i*, μm
d_{CP} = average size of CP, μm
F_b = granular particle influence factor (the influence of particles size and the weight percent of the residual catalyst to the electrostatic potentials in the fluidized bed)
F_b' = particle size influence factor
F_b'' = residual catalyst influence factor
H_e = measurement point height, mm
i = type of the granular polyethylene, $i = 1, 2, 3, 4$
MI = melting index of LLDPE particles, g·(10 min^{-1})
U_0 = electrostatic potential with only CP polyethylene, V
U = electrostatic potential with GP*i* polyethylene added, V
ρ = density of the LLDPE particles, g·cm^{-3}
ω_{GPi} = weight percent of the GP*i* polyethylene, %
ω_{CP} = weight percent of the CP polyethylene, %

Literature Cited

(1) Cross, J. A. *Electrostatics: Principles, Problems and Applications*; Adam Higler: Bristol, U.K., 1987.

(2) Meier, G. B.; Weickert, G.; Swaaij, W. P. M. FER for catalyst propylene polymerization: Controlled mixing and reactor modeling. *AIChE J.* **2003**, *48* (6), 1268–1283.

(3) Lewis, W. K.; Gilliland, E. R.; Bauer, W. C. Characteristics of fluidized particles. *Ind. Eng. Chem.* **1949**, *41*, 1104–1117.

(4) Miller, C. O.; Longwinuk, A. K. Fluidization studies of solid particles. *Ind. Eng. Chem.* **1951**, *43*, 1220–1226.

(5) Leva, M. Elutriation of fines from fluidized bed system. *Chem. Eng. Progr.* **1951**, *47*, 39–45.

(6) Osberg, G. L.; Charlesworth, O. H. Electrization in a fluidized bed. *Chem. Eng. Progr.* **1951**, *47*, 566–570.

(7) Soo, S. L. Electrostatic hazards in pneumatic conveying. *J. Pipelines* **1981**, *1*, 57–68.

(8) Nieh, S.; Nguyen, T. Effects of humidity, conveying velocity, and particles size on electrostatic charges of glass beads in a gaseous suspensions flow. *J. Electrostatics* **1988**, *21*, 9–114.

(9) Ciborawski, J.; Woldarski, A. On electrostatic effects in fluidized beds. *Chem. Eng. Sci.* **1962**, *17*, 23–32.

(10) Boland, D.; Geldart, D. Electrostatic charging in gas fluidized beds. *Powder Technol.* **1971/1972**, *5*, 289–297.

(11) Baily, A. G. Electrostatic phenomena during powder handling. *Powder Technol.* **1984**, *37*, 71–85.

(12) Astbury, G. R.; Harper A. J. Large-Scale Chemical Plants: Eliminating the Electrostatic Hazards. *Electrostatics, 1999: Proceedings of the 10th International Conference*, Cambridge, U.K.; 1999; pp 207−210.

(13) Jones, T. B. Electrostatics and Dust Explosions in Powder Handling. In *Selected Topics on Fluidization, Solid Handling, and Processing*: Yang, W. C., Ed.; Noyes: Park Ridge, NJ, 1999: pp 817−871.

(14) Park, A.; Bi, H.; Grace, J. R. Reduction of electrostatic charges in gas-solid fluidized beds. *Chem. Eng. Sci.* **2002**, *57* (1), 153–162.

(15) Guradiola, J.; Rojo, V.; Ramos, G. Influence of particles velocity and relative humidity on fluidized bed electrostatics. *J. Electrostatics* **1996**, *37*, 1–20.

(16) Ali, F. S.; Inculet, I. I.; Tedoldi, A. Charging of polymer powder inside a metallic fluidized bed. *J. Electrostatics* **1999**, *45*, 199–211.

(17) Ali, F. S.; Ali, M. A.; Ali, R. A.; Inclulet, I. I. Minority charge separation in falling particles with bipolar charge. *J. Electrostatics* **1998**, *45*, 139–155.

(18) Zhao, H.; Castle, G. S. P.; Inculet, I. I.; Bailey, A. G. Bipolar charging of poly-disperse polymer powders in fluidized beds. *IEEE Trans. Ind. Appl.* **2003**, *39*, 612–618.

(19) Stow, C. D. Atmospheric electricity. *Rep. Prog. Phys.* **1969**, *32*, 1–67.

(20) Crozier, W. D. The electric field of a New Mexico dust devil. *J. Geophys. Res.* **1964**, *69*, 5427.

(21) Ette, A. I. I. The effect of the Harmattan dust on atmospheric electric parameters. *J. Atmos. Terr. Phys.* **1971**, *33*, 295–300.

(22) Melnik, O.; Parrot, M. Electrostatic discharge in Martian dust storms. *J. Geophys. Res.* **1998**, *103*, 29107–29118.

(23) Steve, T.; Nick, G.; Yurteri, C. U. Effects of surface properties on the tribocharging characteristics of polymer powder as applied to industrial processes. *IEEE Trans. Ind. Appl.* **2003**, *39*, 79–86.

(24) Zhao, H.; Castle, G. S. P.; Inculet, I. I. The measurement of bipolar charge in polydisperse powders using a vertical array of Faraday pail sensors. *J. Electrostatics* **2002**, *55*, 261–278.

(25) Rojo, V.; Guardiola, J.; Vian, A. A capacitor model to interpret the electric behaviour of fluidized beds. Influence of apparatus geometry. *Chem. Eng. Sci.* **1986**, *41*, 2171–2181.

(26) Fulks, D. B.; Sawin, S. P.; Aikman, C. D.; Jenkins J. M. *Process for reducing sheeting during polymerization of alpha-olefins*. U.S. Patent 4,876,320, 1989.

(27) Goode, M. G.; Williams, C. C.; Hussein F. D.; McNeil T. J.; Lee K. H. *Static control in olefin polymerization*. U.S. Patent 61,110,344, 2000.

(28) Wolny, A.; Opalinski, I. Electric charge neutralization by addition of fines to a fluidized bed composed of coarse dielectric particles. *J. Electrostatics* **1983**, *14* (3)), 279–289.

(29) Wolny, A.; Kazmierczak, W. Triboelectrification in fluidized bed of polystyrene. *Chem. Eng. Sci.* **1989**, *44* (11), 2607–2610.

(30) Park, A.; Bi, H.; Grace, J. R. Reduction of electrostatic charges in gas-solid fluidized beds. *Chem. Eng. Sci.* **2002**, *57* (1), 153–162.

(31) Mehrani, P.; Bi, H. T.; Grace, J. R. Electrostatic behavior of different fines added to a Faraday cup fluidized bed. *J. Electrostatics.* **2007**, *65* (1), 1–10.

(32) Ferrero, M. A.; Chiovetta, M.G. Catalyst fragmentation during propylene polymerization: Part I. The effects of grain size and structure. *Polym. Eng. Sci.* **1987**, *27*, 1436–1447.

(33) Park, A.-H. A.; Bi, H. T.; Grace, J. R.; Chen, A. Modeling charge transfer and induction in gas-solid fluidized beds. *J. Electrostatics* **2002**, *55* (1), 135–158.

(34) Brown, R. L.; Richard, J. C. *Principles of Powder Mechanics*; Pergamon Press: New York, 1970.

(35) Deriaguin, B.; Krotiva, N.; Smilga, W. *Adhesion of Solids*; Izd "Nauka": Moscow, 1977.

(36) Elsdon, R.; Mitchell, F. R. G. Contact electrification of polymers. *J. Phys. D: Appl. Phys.* **1976**, *9*, 1445–1460.

(37) Ahuja, S. K. A collision model of charge exchange between metal and polymer spheres. *J. Phys. D: Appl. Phys.* **1976**, *9*, 1305–1314.

(38) Inculet, I. I.; Castle, G. S. P.; Aartsen, G. Generation of bipolar electric fields during industrial handling of powders. *Chem. Eng. Sci.* **2006**, *61* (7), 2249–2253.

Received for review November 10, 2008
Revised manuscript received October 26, 2009
Accepted November 10, 2009

IE8017077